IEICE TRANS. ELECTRON., VOL.E105–C, NO.10 OCTOBER 2022

INVITED PAPER *Special Section on Microwave and Millimeter-Wave Technologies*

Surrogate-Based EM Optimization Using Neural Networks for Microwave Filter Design

Masataka OHIRA[†a)], ***Member and*** **Zhewang MA**[†], ***Senior Member***

SUMMARY A surrogate-based electromagnetic (EM) optimization using neural networks (NNs) is presented for computationally efficient microwave bandpass filter (BPF) design. This paper first describes the forward problem (EM analysis) and the inverse problems (EM design), and the two fundamental issues in BPF designs. The first issue is that the EM analysis is a time-consuming task, and the second one is that EM design highly depends on the structural optimization performed with the help of EM analysis. To accelerate the optimization design, two surrogate models of forward and inverse models are introduced here, which are built with the NNs. As a result, the inverse model can instantaneously guess initial structural parameters with high accuracy by simply inputting synthesized coupling-matrix elements into the NN. Then, the forward model in conjunction with optimization algorithm enables designers to rapidly find optimal structural parameters from the initial ones. The effectiveness of the surrogate-based EM optimization is verified through the structural designs of a typical fifth-order microstrip BPF with multiple couplings.

key words: *microstrip filters, neural networks, surrogate models, electromagnetic optimization*

1. Introduction

As the demand for wireless communications increases, electromagnetic (EM) circuit designs rely more and more heavily on commercially available EM simulators in the last few decades. Complicated and time-consuming EM design tasks may stem from a fundamental issue that an *inverse problem* of EM circuit cannot be directly solved by any analytical or numerical approach at this time. Here the inverse problem is to find an optimal physical circuit from a given electrical response. Therefore, circuit designers are forced to find optimal structural parameters by repeatedly updating the parameters while solving the *forward problem* of EM circuit through the EM simulator. The forward model in EM problems is to calculate an electrical response, i.e. S-parameters, from a given physical circuit through an EM analytical method such as the finite-element method [1] and the method of moments [2].

As a matter of course, microwave bandpass filter (BPF) design definitely faces the same difficulty. Fortunately, the filter circuit synthesis theory [3], [4], which determines the circuit topology and its parameters from a given transfer function, is well established and is widely used in microwave community. This means that the filter circuit can be synthesized by solving the inverse problem of filter circuit. However, the physical filter structure and its dimensions need to be designed with the aid of EM simulator so as to acquire the synthesized circuit parameters [4], [5], because any EM effects like fringing effects and frequency dispersion are not considered in the equivalent circuit.

To bridge the gap between the physical structure and the equivalent circuit, optimization algorithms including local and global search optimizations have been utilized in EM circuit designs. Novel EM optimization approaches, such as EM design combined with genetic algorithm (GA), have been vigorously developed so far [6]–[9]. In such optimization designs, one of the bottlenecks is the computation time of EM analysis or EM simulation. In the local search optimization, on the other hand, designers may make an extraordinary effort to find good initial structural parameters, which is important to get a faster convergence in iterative approaches. To tackle the problem of the computation time, the concept of *surrogate*-based EM optimization has been introduced into filter designs. One of well-known approaches is a space-mapping method [10]–[12], which offers a mathematical link between coarse and fine models and provides fast computations using the coarse model (equivalent circuit or empirical model) with keeping computational accuracy by the corresponding time-intensive fine model (EM simulation). However, this method requires appropriate coarse models.

In recent years, neuro-based surrogate models have gained much attention [13]–[27] because neural networks (NNs) has made remarkable progress. The NN can easily model the relationship between input and output using a dataset prepared in advance. Furthermore, the NN offers fast computation once it is constructed. Therefore, an electrical response can be obtained incomparably faster than EM simulation just by inputting structural parameters of BPF into the NN. Such a surrogate model may be called *forward model*, since the relationship between input and output is the same as the forward problem of EM analysis. On the other hand, a surrogate model with the opposite input-output relationship with respect to the forward model is referred to as *inverse model*. By simply reversing the input and output of the dataset, we can build the inverse model using NN. The introduction of the inverse model allows us to directly obtain structural parameters just by inputting an electrical response into NN [20], [21]. The authors have proposed a novel NN-based inverse model [23], of which the input is coupling matrix elements and the output is structural parameters of BPF.

Manuscript received January 27, 2022.
Manuscript revised February 22, 2022.
Manuscript publicized March 15, 2022.

[†]The authors are with Graduate School of Science and Engineering, Saitama University, Saitama-shi, 338–8570 Japan.
a) E-mail: mohira@mail.saitama-u.ac.jp

DOI: 10.1587/transele.2022MMI0005

The inverse model cannot necessarily find optimal solutions to meet design specifications, especially for a higher-order BPF, because a one-to-one mapping between input and output is not always guaranteed in the inverse model, unlike the forward one.

This paper presents a novel EM optimization design approach of a higher-order microstrip BPF using both forward and inverse models constructed by NNs [25]. In the first design stage, the inverse model in the proposed design method is employed for initial guess of structural parameters of BPF. The inverse model can find a solution very close to optimal one, even for a higher-order BPF. In the second design stage, optimal structural parameters can be obtained by a structural optimization through iterative evaluations of S-parameters using the forward model. These two design stages are instantly and smoothly executed by NNs without any manual tunings. The effectiveness of the surrogate-based EM optimization presented in this paper is demonstrated through design examples of a fifth-order microstrip BPF.

2. Forward and Inverse Problems: EM Analysis and Design

2.1 Forward and Inverse Problems

This section revisits the forward and inverse problems in EM circuits. As shown in Fig. 1, in general, the *circuit analysis* is to calculate electrical parameters $\mathbf{y}$ from circuit parameters $\mathbf{x}$ as

$$\mathbf{y} = \mathbf{f}_{\text{for}}(\mathbf{x}) \tag{1}$$

where $\mathbf{f}_{\text{for}}$ expresses the relationship between the input vector $\mathbf{x}$ and the output one $\mathbf{y}$ in this forward problem. On the other hand, the *circuit synthesis* is to obtain a circuit topology and its parameters $\mathbf{x}$ from electrical parameters $\mathbf{y}$ by

$$\mathbf{x} = \mathbf{f}_{\text{inv}}(\mathbf{y}) \tag{2}$$

where $\mathbf{f}_{\text{inv}}$ denotes the input/output relationship in the inverse problem. In the filter design, the filter circuit synthesis theory has already been established to determine the circuit configuration and circuit parameters that give a desired frequency response [3], [4]. The synthesized circuit is an equivalent circuit of filter. The filter, in practice, is realized by a physical circuit such as microstrip lines and waveguides. Therefore, the EM analysis is indispensable to calculating frequency responses of the physical circuit by solving Maxwell's equations under boundary conditions. For the last few decades, EM simulators have been widely used for this purpose. Needless to say, the EM analysis or EM simulation is the *forward problem*, whereas the EM design of the physical circuit is the *inverse problem*.

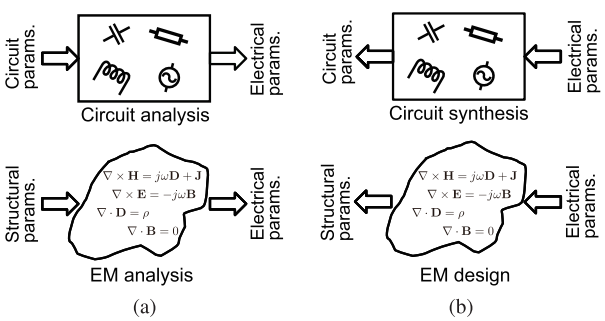

Fig. 1 (a) Forward problems in EM and circuit analyses. (b) Inverse problems in circuit synthesis and EM design.

However, there is no straightforward way to directly obtain optimal physical structure from a desired frequency response. In other words, the inverse problem of the EM circuit is considered to be unsolvable. Therefore, we are forced to use an EM simulator over and over again to evaluate the frequency response of physical circuit every time the structural parameters are adjusted. This leads to a huge amount of computational time in EM design.

2.2 Forward and Inverse Models

To solve the abovementioned issue in the EM design, two surrogate models are introduced in Fig. 2. One is the forward model to calculate electrical parameters $\mathbf{y}_{\text{for}}$ from structural parameters $\mathbf{x}_{\text{for}}$ by

$$\mathbf{y}_{\text{for}} = \bar{\mathbf{f}}_{\text{for}}(\mathbf{x}_{\text{for}}) \tag{3}$$

as a substitute for EM analysis. The other is the inverse model to find structural parameters $\mathbf{y}_{\text{inv}}$ from electrical parameters $\mathbf{x}_{\text{inv}}$ with

$$\mathbf{y}_{\text{inv}} = \bar{\mathbf{f}}_{\text{inv}}(\mathbf{x}_{\text{inv}}) \tag{4}$$

In Eq. (3) and (4), $\bar{\mathbf{f}}_{\text{for}}$ and $\bar{\mathbf{f}}_{\text{inv}}$ express the input/output relationship of the forward and inverse models, respectively.

The forward model offers a fast computation with the accuracy enough for design, instead of using EM simulators, but optimal structural parameters cannot be found only with the forward model. In contrast, the inverse model has a possibility that it becomes a true design tool since it can directly solve the inverse problem. However, the existence and the uniqueness of solutions are not guaranteed in general. A surrogate-based EM optimization compensates for the shortcomings of both models, which will be explained in the next section.

3. Surrogate-Based EM Optimization for BPF Design

3.1 Design Flow and Surrogate Models

The surrogate-based EM optimization for BPF design has

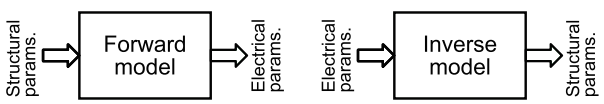

Fig. 2 Surrogate models. (a) Forward model for EM analysis and (b) inverse model for EM design.

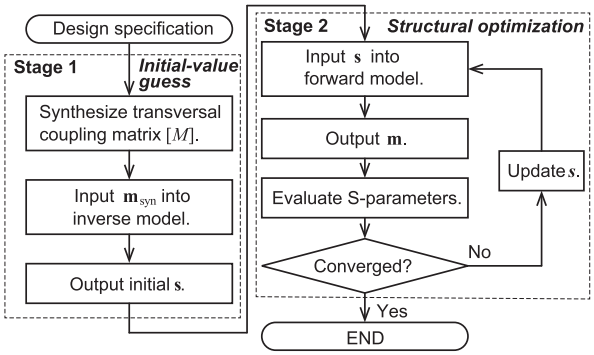

Fig. 3 Procedure of surrogate-based EM optimization for BPF design.

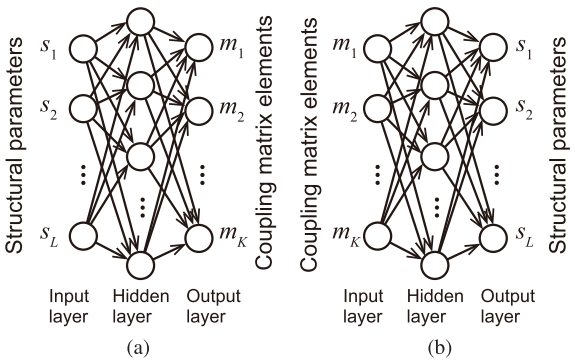

Fig. 4 Surrogate models using neural networks for BPF design. (a) Forward model and (b) inverse model.

two stages, as shown in Fig. 3. The first stage is finding initial values of structural parameters. The second stage is optimizing structural parameters from their initial values so that requirements of filter response can be met. These two design stages may be totally the same as a well-known BPF design approach, but they are performed by two surrogate models of forward and inverse models. This is the reason why the flowchart given in Fig. 3 is called surrogate-based EM optimization. In this work, the two surrogate models are constructed by NNs, significantly reducing computational burden in the optimization process.

The two surrogate models used in this work are given in Fig. 4. They have two vectors: one is the vector consisting of structural parameters as

$$\mathbf{s} = [s_1 \; s_2 \; \cdots \; s_L]^T \tag{5}$$

where L is the number of structural parameters, and T stands for the transposed vector. The other is the vector of coupling matrix elements

$$\mathbf{m} = [m_1 \; m_2 \; \cdots \; m_K]^T \tag{6}$$

in the lowpass-prototype frequency domain [28], where K is the number of coupling matrix elements. In the forward model, the input vector $\mathbf{x}_{\text{for}}$ is $\mathbf{s}$ and the output one $\mathbf{y}_{\text{for}}$ is $\mathbf{m}$. In the inverse model, the input vector $\mathbf{x}_{\text{inv}}$ is $\mathbf{m}$ and the output one $\mathbf{y}_{\text{inv}}$ is $\mathbf{s}$. Each model is expressed with a well-known NN having input, hidden, and output layers.

3.2 Initial-Value Guess Using Inverse Model

The initial-value guess of structural parameters is done by the inverse model given in Fig. 4 (b). By inputting ideal coupling matrix elements $\mathbf{m}_{\text{sys}}$ into the inverse model, a set of structural parameters $\mathbf{s}$ is instantaneously obtained from the NN. The ideal coupling-matrix elements can be synthesized by the filter circuit synthesis theory [28]. In a conventional filter design approach [5], resonator lengths and gaps need to be individually designed without considering intrinsically generated cross couplings between resonators. Such effects are incorporated in the inverse model given in Fig. 4 (b), of which the detail will be described later. However, the inverse model cannot always find optimal structural parameters from ideal coupling-matrix elements, owing to inherent nature of inverse problem. Moreover, a physical filter structure to be designed cannot support all ideal frequency responses. Nevertheless, this inverse model can output nonoptimal yet extremely good initial values without depending on filter designers' experience. This is of utmost importance for EM optimization using local search algorithms to ensure fast convergence in the next design stage.

3.3 Structural Optimization Using Forward Model

The second stage is the structural optimization assisted by the forward model. The forward model plays a crucial role for the calculation of S-parameters. By inputting a set of structural parameters $\mathbf{s}$ into the forward model, the NN can instantly output the corresponding coupling matrix elements $\mathbf{m}$. Then, S-parameters can be quickly calculated from the coupling matrix $[M]$ with algebraic computation [28]. No EM simulators are needed in the two design stages once the two NNs are constructed. The structural parameters are optimized starting from the initial values estimated at the first design stage. Thanks to good initial-value guess, they rapidly converge to optimal values through a local search algorithm. In the next section, it will be addressed why the surrogate models constructed by the NN make it possible to effectively and accurately design the BPF even if the BPF has multiple cross couplings.

4. Building Neural Networks for Forward and Inverse Models

4.1 Circuit Modeling of Multicoupled BPF

As shown in Fig. 4, the NN used for the forward and inverse models provides an approximated function connecting structural parameters of BPF with electrical ones of coupling matrix [23].

In the two surrogate models, the BPF is modeled by a transversal resonator array circuit [28], which is now known as a general equivalent circuit of coupled-resonator filters. The transversal coupling matrix is expressed by

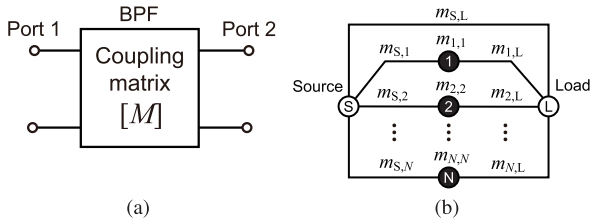

(a) (b)

Fig. 5 (a) Black-box macromodeling of BPF. (b) Transversal coupling topology of coupled-resonator filter. While and black circles represent non-resonant and resonant nodes, respectively. Lines connecting nodes express couplings.

$$[M] = \left[\begin{array}{c|ccccc} 0 & m_{\mathrm{S},1} & m_{\mathrm{S},2} & \cdots & m_{\mathrm{S},N} & m_{\mathrm{S,L}} \\ \hline m_{\mathrm{S},1} & m_{1,1} & 0 & \cdots & 0 & m_{1,\mathrm{L}} \\ m_{\mathrm{S},2} & 0 & m_{2,2} & \cdots & 0 & m_{2,\mathrm{L}} \\ \vdots & \vdots & \vdots & \ddots & \vdots & \vdots \\ m_{\mathrm{S},N} & 0 & 0 & \cdots & m_{N,N} & m_{N,\mathrm{L}} \\ \hline m_{\mathrm{S,L}} & m_{1,\mathrm{L}} & m_{2,\mathrm{L}} & \cdots & m_{N,\mathrm{L}} & 0 \end{array}\right] \tag{7}$$

in the normalized frequency domain of lowpass prototype filter. Here the subscripts S, L, and i ($i = 1, 2, \cdots, N$) denote source, load, and a resonator number, respectively, where N is the number of resonators.

Figure 5 shows a transversal coupling configuration formed by parallelly connected resonators. The resonators in this filter configuration are interpreted not as physical one but as eigenmode resonances of coupled resonators [29]. All the inter-resonator couplings of Nth-order filter are expressed by N eigenmode resonances appearing in filter. That is to say, undesired but non-negligible cross couplings are fully taken into consideration in the transversal coupling. If the transversal coupling matrix is employed for the circuit modeling of BPF, filter designers do not necessarily need to know exactly how resonators are coupled to each other in the physical filter circuit.

4.2 Generation of Dataset

To build the forward and inverse models using the NN, the dataset composed of a pair of **s** and **m** is prepared in advance. The dataset can be generated with the help of a parametric sweep function of a commercially available EM simulator. First, a variable range $[s_{i,\min},\ s_{i,\max}]$ of each structural parameter s_i ($i = 1, 2, \cdots, L$) to be designed is given, and then the S-parameters are calculated with the EM simulator for every set of structural parameters in a parameter space defined. After that, the transversal coupling matrix $[M]$ or its matrix elements **m** are extracted from the EM-simulated S-parameters with a parameter-extraction technique [30]. Interestingly, any pre-designed BPF results are not needed for the dataset.

Each structural parameter is normalized for efficiently constructing the NN by

$$\bar{s}_i = \frac{s_i - s_{i,\min}}{s_{i,\max} - s_{i,\min}}. \tag{8}$$

In the next section, the denormalized structural parameters will be given for a better understanding of filter layout.

On the other hand, the extracted coupling-matrix elements are also normalized using a arbitrary center angualr frequency $f_{0,\mathrm{data}}$ and fractional bandwidth $\mathrm{FBW}_{\mathrm{data}}$ by [24]

$$m_{i,i} = -\frac{\Omega_c}{\mathrm{FBW}_{\mathrm{data}}}\left(\frac{\omega_{0i}}{\omega_{0,\mathrm{data}}} - \frac{\omega_{0,\mathrm{data}}}{\omega_{0i}}\right) \tag{9}$$

$$m_{\mathrm{S},i} = \sqrt{\frac{\Omega_c}{\mathrm{FBW}_{\mathrm{data}} \cdot Q_{\mathrm{ext},i}}} \tag{10}$$

$$m_{i,\mathrm{L}} = \begin{cases} m_{\mathrm{S},i} & \text{for even mode} \\ -m_{\mathrm{S},i} & \text{for odd mode} \end{cases} \tag{11}$$

where ω_{0i} and $Q_{\mathrm{ext},i}$ for $i = 1, 2, \cdots, N$ represent the extracted resonant angular frequency and external Q factor, respectively; Ω_c is the cutoff angular frequency in the lowpass prototype frequency domain, which is normally 1. The synthesized coupling matrix elements will be presented with the above normalized values.

4.3 Supervised Learning

The two NNs for the forward and inverse models are separately constructed with a supervised learning using the same dataset of **s** and **m**. As described in the previous section, the input and output vectors of the forward model are **s** and **m**, respectively, and vice versa for the inverse model. Each NN is trained with an error backpropagation algorithm [13], until the mean squared error (MSE) is enough small to design the structural parameters of BPF. The MSE is defined by

$$\mathrm{MSE} = \frac{1}{N_{\mathrm{data}} N_{\mathrm{out}}} \sum_{t=1}^{N_{\mathrm{data}}} \sum_{k=1}^{N_{\mathrm{out}}} (y_{k,t} - d_{k,t})^2 \tag{12}$$

where N_{data} and N_{out} denote the number of data prepared in advance and the output nodes in the NN, respectively; $y_{k,t}$ is kth element of the output from the NN when tth dataset is input into the NN; $d_{k,t}$ is the training data prepared in advance. The next section demonstrates a microstrip BPF design through the surrogate-based EM optimization.

5. Design Examples

5.1 Microstrip Filter Structure

As an example, a microstrip BPF shown in Fig. 6 is designed by the surrogate-based EM optimization technique. The BPF has a typical symmetric filter structure that can be found in textbooks. However, it may be hard to obtain an ideal passband response with conventional design methods owing to unexpected cross couplings, resulting in the generation of transmission zero (TZ) at stopband.

The BPF has six structural parameters l_1, l_2, l_3, g_1, g_2, and l_{q} to be designed on a dielectric substrate of relative permittivity $\varepsilon_r = 2.6$ and thickness $t = 1.0$ mm. The width w of resonators is fixed to be 2.00 mm. The material losses

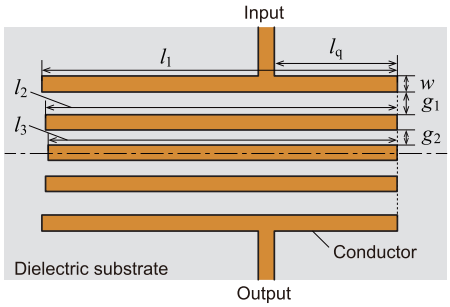

Fig. 6 Top view of fifth-order microstrip BPF layout to be designed.

and radiation loss are neglected in this demonstration for simplicity.

5.2 Building Surrogate Models

5.2.1 Generation of Dataset

Next, the training data is prepared to construct the surrogate models in the parameter space of $33.00 \le l_1, l_2, l_3 \le 35.00$, $1.50 \le g_1, g_2 \le 4.00$, and $11.00 \le l_q \le 13.00$ in mm with 0.5-mm step. The validation data is also generated in the ranges of the parameter space of $33.25 \le l_1, l_2, l_3 \le 34.75$, $1.75 \le g_1, g_2 \le 3.75$, and $11.25 \le l_q \le 12.75$ in mm with 0.5-mm step. These variable ranges of the structural parameters are roughly estimated from design specifications (center frequency 3 GHz) described later. However, since the number of all combinations is very large, the variable ranges of resonator lengths are limited to the case of $l_1 \ge l_2 \ge l_3$. This is because it is empirically known that designed structural parameters may be fallen into the ranges of $l_1 \ge l_2 \ge l_3$ in the case of BPF shown in Fig. 6. As a result, the numbers of training and validation data are 6300 and 2000, respectively, in this demonstration. The S-parameters used for the dataset are calculated with the EM simulator Sonnet *em*.

5.2.2 Building Neural Networks

The dataset in the design examples has a pair of the following $\boldsymbol{s}$ and $\boldsymbol{m}$.

$$\mathbf{s} = [l_1\ l_2\ l_3\ g_1\ g_2\ l_q]^T \tag{13}$$

$$\mathbf{m} = [m_{S,1}\ m_{S,2}\ m_{S,3}\ m_{S,4}\ m_{S,5}\ m_{1,1}\ m_{2,2}\ m_{3,3}\ m_{4,4}\ m_{5,5}]^T \tag{14}$$

where $m_{i,L}$ $(i = 1, 2, \cdots, 5)$ is omitted from $\mathbf{m}$ because of the relationship between in $m_{S,i}$ and $m_{i,L}$ in Eq. (11). $m_{S,L}$ is also unused because it does not significantly affect the passband response. In the forward model, the input into the NN is $\mathbf{x}_{for} = \mathbf{s}$ and the output from the NN is $\mathbf{y}_{for} = \mathbf{m}$, while the input is $\mathbf{x}_{inv} = \mathbf{m}$ and the output is $\mathbf{y}_{inv} = \mathbf{s}$ in the inverse model. In this BPF design, the absolute value of S_{11} in passband needs to be calculated to about two decimal places. To this end, the convergence goal of MSE of the output $\mathbf{y}_{for} = \mathbf{m}$ in Eq. (12) is set to 10^{-4} or less. In the inverse model, the structural parameters $\mathbf{s}$ are designed with 0.05-mm step, which is the cell size used in the EM simulator Sonnet *em* for this microstrip BPF, so that the MSE of the output $\mathbf{y}_{inv} = \mathbf{s}$ (in mm) in Eq. (12) is required to be converged to less than about 10^{-4}.

The NNs to be built for the forward and inverse models has basic three layers of input, hidden, and output layers. The number of hidden layers is one, since the goal of the MSE can be achieved. In the NNs, the sigmoid function is chosen as the activation function because we confirmed that there are no significant differences even when the activation function is changed to other one. The number of units in the hidden layers is set to 60 in the forward model and 70 in the inverse model, so that the MSE of both training and validation data can be minimized. In the forward and inverse models, the resultant MSEs of the training data are 3.9×10^{-5} and 9.2×10^{-5}, respectively, while those of the validation data are 7.7×10^{-5} and 9.8×10^{-5}, respectively. Each value is less than the target MSE.

5.3 EM Optimization Design Using Surrogate Models

The surrogate-based EM optimization for the BPF design is performed using the constructed forward and inverse models. In this section, three microstrip BPFs are designed under the following specifications. The specifications common to the three designs are as follows.

- Number of resonators: $N = 5$
- Transfer function: generalized Chebyshev function
- TZ frequency: $f_{TZ} = 3.15$ GHz

In the same parameter space as the dataset, the same forward and inverse models are employed for three designs. The TZ frequency is included in the specification since one TZ are generated at upper stopband because of couplings between non-adjacent resonators in the BPF shown in Fig. 6. The purpose of adding the TZ frequency is not to generate the TZ at the specified frequency, but to estimate the initial structural parameters with the inverse model. The passband responses of the three designs A, B, and C are listed below.

Design A:

- Center frequency: $f_0 = 3.00$ GHz
- Fractional bandwidth: FBW = 5 %
- In-band return loss: $R_L \ge 20$ dB

Design B:

- Center frequency: $f_0 = 3.00$ GHz
- Fractional bandwidth: FBW = 4 %
- In-band return loss: $R_L \ge 25$ dB

Design C:

- Center frequency: $f_0 = 2.95$ GHz
- Fractional bandwidth: FBW = 6 %
- In-band return loss: $R_L \ge 20$ dB

The aim of the design examples is to form the specified

Table 1 Initial and optimized structural parameters.

Struc. params	Design A		Design B		Design C	
	Initial (mm)	Optimized (mm)	Initial (mm)	Optimized (mm)	Initial (mm)	Optimized (mm)
l_1	34.05	34.05	34.05	34.10	34.65	34.65
l_2	33.55	33.45	33.55	33.50	34.20	34.05
l_3	33.40	33.45	33.45	33.50	33.95	34.00
g_1	2.15	2.15	2.45	2.55	1.65	1.70
g_2	3.25	3.10	3.70	3.60	2.85	2.60
l_q	12.80	12.70	12.85	12.85	12.80	12.75

passband. Therefore, the passband response is evaluated by the objective function in the structural optimization. The objective function F is defined by

$$F = \sum_{k=1}^{N_s} \left(\left| \bar{S}_{11}(f_k) \right| - \left| S_{11}^{(\text{ideal})}(f_k) \right| \right)^2 \tag{15}$$

In Eq. (15), $\bar{S}_{11}$ is the reflection coefficient calculated from the coupling matrix output by the forward model at a sampling frequency f_k ($k = 1, 2, \cdots, N_s$), where N_s is the number of sampling frequencies. $S_{11}^{(\text{ideal})}$ represents a target reflection coefficient that can be calculated from a coupling matrix synthesized from the design specification. The frequency range and the number of sampling frequencies are 2.925–3.075 GHz and $N_s = 301$ for the design A, 2.94–3.06 GHz and $N_s = 241$ for the design B, and 2.8615–3.0385 GHz and $N_s = 355$ for the design C, respectively.

The synthesized coupling matrix elements $\mathbf{m}_{\text{syn}}$ are obtained from the above specifications of the designs A, B, and C as

$$\text{A: } \mathbf{m}_{\text{syn}} = [0.374 \;\; 0.521 \;\; 0.317 \;\; 0.537 \;\; 0.474 \;\; 1.276 \;\; -0.172 \;\; -1.206 \;\; 0.783 \;\; -0.957]^T \tag{16}$$

$$\text{B: } \mathbf{m}_{\text{syn}} = [0.417 \;\; 0.561 \;\; 0.371 \;\; 0.587 \;\; 0.432 \;\; 1.407 \;\; -0.154 \;\; -1.322 \;\; 0.904 \;\; -1.049]^T \tag{17}$$

$$\text{C: } \mathbf{m}_{\text{syn}} = [0.372 \;\; 0.520 \;\; 0.322 \;\; 0.533 \;\; 0.478 \;\; 1.273 \;\; -0.151 \;\; -1.212 \;\; 0.793 \;\; -0.945]^T \tag{18}$$

Inputting $\mathbf{m}_{\text{syn}}$ into the inverse model as $\mathbf{x}_{\text{inv}}$, the output $\mathbf{y}_{\text{inv}}$ or the initial structural parameters $\mathbf{s}$ are instantly obtained as shown in Table 1. After optimizing the structural parameters using the quasi-Newton method in conjunction with the forward model, the optimized values shown in Table 1 are acquired within about 10 iterations. The values of all structural parameters shown in Table 1 are rounded to 0.05 mm†. It takes less than about 20–40 seconds (CPU: Intel Xeon 3.4 GHz) to get the optimized values, even though the forward model is repeatedly called in the optimization process for the calculation of function values and derivatives in our homemade program. Furthermore, it must be emphasized in Table 1 that the initial values are very close to the optimized ones, which suggests that the initial-value guess by the inverse model works very well. The uniqueness of solution in the inverse model is not a problem in these designs because a parameter space is not so wide.

†0.05 mm comes from the cell size used in the EM simulator. The values less than 0.05 mm are interpolated by the NNs.

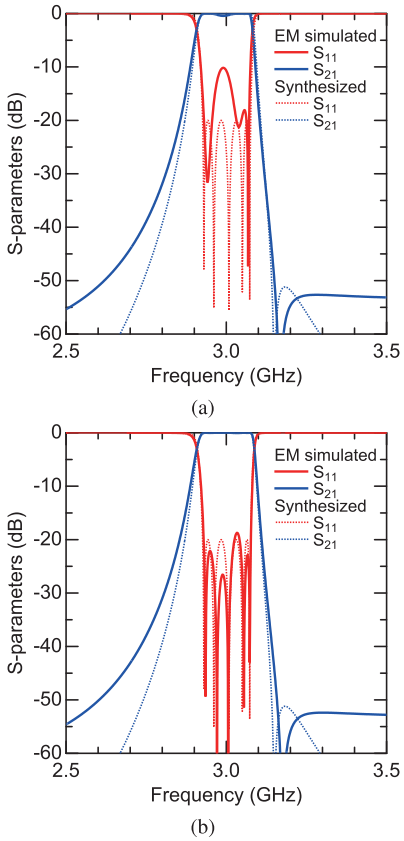

Fig. 7 Comparison of frequency responses between EM-simulated results and theoretical ones of synthesized coupling matrix (design A). (a) Initial structural parameters and (b) optimized ones.

Figures 7, 8, and 9 show the comparison of frequency responses between EM simulation results of the designed filters and the theoretical ones of the synthesized coupling matrices for the designs A, B, and C, respectively. In each figure, the frequency responses with initial and optimized structural parameters are plotted. Although the return loss level of the initial structural parameters is not suppressed as specified, it is clearly improved after the structural optimization, and five reflection zeros successfully appear in the passband. Some discrepancies between the synthesized S_{11} and the optimized one are observed, especially in the design B. In general, as the bandwidth becomes narrower, the higher design accuracy of structural parameters is needed. In the design B with the narrowest bandwidth, a finer parameter step may be required to meet the specification. Nonetheless, these design results support that once the forward and inverse models are constructed, the structural optimization is drastically accelerated by the forward and inverse models using the NNs.

6. Conclusion

A new surrogate-based EM optimization using the NNs has

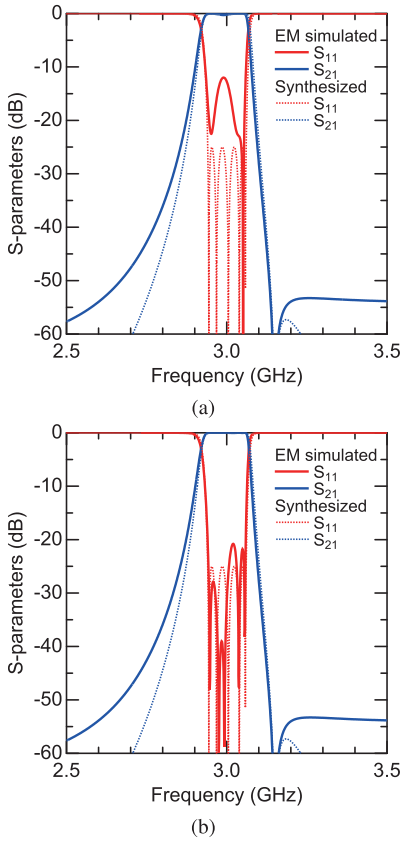

Fig. 8 Comparison of frequency responses between EM-simulated results and theoretical ones of synthesized coupling matrix (design B). (a) Initial structural parameters and (b) optimized ones.

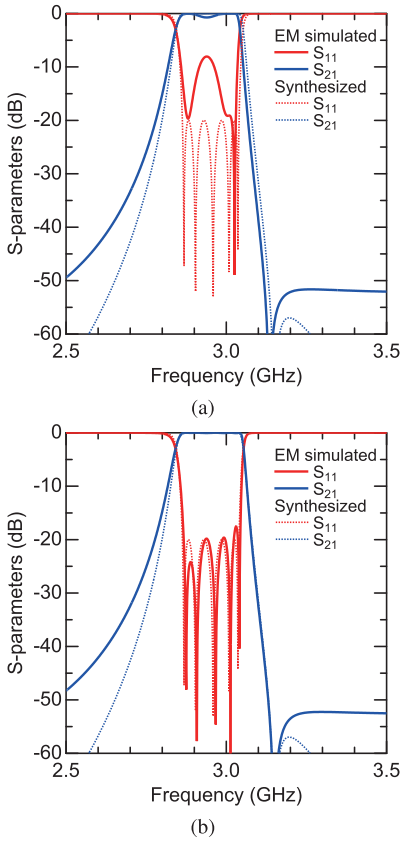

Fig. 9 Comparison of frequency responses between EM-simulated results and theoretical ones of synthesized coupling matrix (design C). (a) Initial structural parameters and (b) optimized ones.

been demonstrated for the microwave filter design. In conventional filter designs, each initial structural parameter is estimated by filter designers, and the structural parameters are adjusted with the aid of time intensive EM simulations. For fast computation, the two surrogate models of forward and inverse models have been introduced in this paper, which have been constructed by the NNs from the dataset simply prepared with the parametric sweep function of EM simulator. The initial structural parameters can be easily found just by inputting the synthesized coupling matrix elements into the inverse model. The structural parameters are rapidly optimized, thanks to the high-speed S-parameter calculation using the forward model, instead of EM simulator. As an example of this design approach, three fifth-order microstrip multicoupled BPFs with different design specifications have been successfully designed, thereby proving the effectiveness of the surrogate-based optimization method.

Acknowledgments

This work was supported in part by JSPS KAKENHI Grant Number 19K04506. The authors would like to thank Mr. Ao Yamashita, Saitama University (now with Mitsubishi Electric) for his significant contributions to this work.

References

[1] J.L. Volakis, A. Chatterjee, and L.C. Kempel, Finite Element Method Electromagnetics: Antennas, Microwave Circuits, and Scattering Applications, Wiley, 1998.
[2] R.F. Harrington, Field Computation by Moment Methods, Wiley, 1993.
[3] G.L. Matthaei, L. Young, and E.M.T. Jones, Microwave Filters, Impedance-Matching Networks, and Coupling Structures, McGraw-Hill, 1964.
[4] R.J. Cameron, C.M. Kudsia, and R.R. Mansour, Microwave Filters for Communication Systems: Fundamentals, Design and Applications (2nd Ed.), Wiley, 2018.
[5] J.-S. Hong, Microstrip Filters for RF/Microwave Applications, 2nd Ed., Wiley, 2011.
[6] J.M. Johnson and V. Rahmat-Samii, "Genetic algorithms in engineering electromagnetics," IEEE Antennas Propag. Mag., vol.39, no.4, pp.7–21, Aug. 1997.
[7] T. Nishino and T. Itoh, "Evolutionary generation of microwave line-segment circuits by genetic algorithms," IEEE Trans. Microw. Theory Tech., vol.50, no.9, pp.2048–2055, Sept. 2002.
[8] T. Nishino and T. Itoh, "Evolutionary generation of 3-D line-segment circuits with a broadside-coupled multiconductor transmission-line model," IEEE Trans. Microw. Theory Tech., vol.51, no.10, pp.2045–2054, Oct. 2003.
[9] M. Ohira, H. Deguchi, M. Tsuji, and H. Shigesawa, "Planar-circuit bandpass filters consisting of arbitrarily shaped elements," Electron. and Commun. in Japan, Part 2, vol.90, no.2, pp.1–8, 2007.
[10] J.W. Bandler, R.M. Biernacki, S.H. Chen, P.A. Grobelny, and

R.H. Hemmers, "Space mapping technique for electromagnetic optimization," IEEE Trans. Microw. Theory Tech., vol.42, no.12, pp.2536–2544, Dec. 1994.
[11] J.W. Bandler, Q.S. Cheng, S.A. Dakroury, A.S. Mohamed, M.H. Bakr, K. Madsen, and J. Sondergaard, "Space mapping: The state of the art," IEEE Trans. Microw. Theory Tech., vol.52, no.1, pp.337–361, Jan. 2004.
[12] J.E. Rayas-Sánchez, "Power in simplicity with ASM: Tracing the aggressive space mapping algorithm over two decades of development and engineering applications," IEEE Microw. Mag., vol.17, no.4, pp.64–76, April 2016.
[13] Q.-J. Zhang, K.C. Gupta, and V.K. Devabhaktuni, "Artificial neural networks for RF and microwave design—From theory to practice," IEEE Trans. Microw. Theory Tech., vol.51, no.4, pp.1339–1350, April 2003.
[14] C. Zhang, J. Jin, W. Na, Q.-J. Zhang, and M. Yu, "Multivalued neural network inverse modeling and applications to microwave filters," IEEE Trans. Microw. Theory Tech., vol.66, no.8, pp.3781–3797, Aug. 2018.
[15] J. Jin, C. Zhang, F. Feng, W. Na, J. Ma, and Q.-J. Zhang, "Deep neural network technique for high-dimensional microwave modeling and applications to parameter extraction of microwave filters," IEEE Trans. Microw. Theory Tech., vol.67, no.10, pp.4140–4155, Oct. 2019.
[16] F. Feng, W. Na, W. Liu, S. Yan, L. Zhu, J. Ma, and Q-J. Zhang, "Multifeature-assisted neuro-transfer function surrogate-based EM optimization exploiting trust-region algorithms for microwave filter design," IEEE Trans. Microw. Theory Tech., vol.68, no.2, pp.531–542, Feb. 2020.
[17] P. Zhao and K. Wu, "Homotopy optimization of microwave and millimeter-wave filters based on neural network model," IEEE Trans. Microw. Theory Tech., vol.68, no.4, pp.1390–1400, April 2020.
[18] O.W. Bhatti, N. Ambasana, and M. Swaminathan, "Design space and frequency extrapolation: Using neural networks," IEEE Microw. Mag., vol.22, no.10, pp.22–36, Oct. 2021.
[19] P. Zhang, Y. Hu, Y. Jin, S. Deng, X. Wu, and J. Chen, "A Maxwell's equations based deep learning method for time domain electromagnetic simulations," IEEE Journal on Multiscale and Multiphysics Computational Tech., vol.6, pp.35–40, 2021.
[20] Y. Wang, M. Yu, H. Kabir, and Q.-J. Zhang, "Effective design of cross-coupled filter using neural networks and coupling matrix," Dig. IEEE MTT-S Int. Microwave Symp., San Francisco, CA, pp.1431–1434, June 2006.
[21] H. Kabir, Y. Wang, M. Yu, and Q.-J. Zhang, "Neural network inverse modeling and applications to microwave filter design," IEEE Trans. Microw. Theory Tech., vol.56, no.4, pp.867–879, April 2008.
[22] T. Akada and K. Fujimori, "Designing microwave circuits using genetic algorithms accelerated by convolutional neural networks," Proc. 50th European Microwave Conference (EuMC), pp.61–64, Jan. 2021.
[23] M. Ohira, A. Yamashita, Z. Ma, and X. Wang, "A novel eigenmode-based neural network for fully automated microstrip bandpass filter design," Dig. 2017 IEEE MTT-S Int. Microwave Symp., Honolulu, HI, June 2017.
[24] A. Yamashita, M. Ohira, Z. Ma, and X. Wang, "A tuning-less design method of microwave bandpass filters using neural network based inverse model," IEICE Trans. Electron. (Japanese Ed.), vol.J101-C, no.8, pp.327–335, Aug. 2018.
[25] M. Ohira, A. Yamashita, Z. Ma, and X. Wang, "Automated microstrip bandpass filter design using feedforward and inverse models of neural network," Proc. 2018 Asia-Pacific Microwave Conf. (APMC), pp.1292–1294, Kyoto, Japan, Nov. 2018.
[26] M. Ohira, "Future microwave circuit design assisted by neural networks – microwave planar filter design as an example –," Rump Session in 2019 Global Symposium on Millimeter Waves (GSMM 2019), Sendai, Japan, May 2019.
[27] M. Ohira, K. Takano, and Z. Ma, "A novel deep-Q-network-based fine-tuning approach for planar bandpass filter design," IEEE Microw. Wirel. Compon. Lett., vol.31, no.6, pp.638–641, June 2021.
[28] R.J. Cameron, "Advanced coupling matrix synthesis techniques for microwave filters," IEEE Trans. Microw. Theory Tech., vol.51, no.1, pp.1–10, Jan. 2003.
[29] S. Amari, "Physical interpretation and implications of similarity transformations in coupled resonator filter design," IEEE Trans. Microw. Theory Tech., vol.55, no.6, pp.1139–1153, June 2007.
[30] M. Ohira and Z. Ma, "A parameter-extraction method for microwave transversal resonator array bandpass filters with direct source/load coupling," IEEE Trans. Microw. Theory Tech., vol.61, no.5, pp.1801–1811, May 2013.

Masataka Ohira received the B.E., M.E., and D.E. degrees from Doshisha University, Kyoto, Japan, in 2001, 2003 and 2006, respectively. From 2006 to 2010, he was with ATR Wave Engineering Laboratories, Kyoto, Japan, where he was engaged in the research and development of millimeter-wave antennas and small smart microwave antennas. He was a Visiting Researcher in ATR Wave Engineering Laboratories for 2010–2011. In 2010, he joined Saitama University, Saitama, Japan, where he is currently an Associate Professor. His current research activities are concerned with the analysis and design of microwave/millimeter-wave filters and antennas. Dr. Ohira is a member of the Institute of Electrical Engineers (IEE) of Japan, European Microwave Association (EuMA), and IEEE. He received the IEICE Young Engineer Award in 2005, IEEE AP-S Japan Chapter Young Engineer Award in 2012, IEEE MTT-S Japan Young Engineer Award, Michiyuki Uenohara Memorial Award in 2014, and IEICE Best Paper Award in 2018.

Zhewang Ma received the B. Eng. and M. Eng. degrees from the University of Science and Technology of China (USTC), Hefei, China, in 1986 and 1989, respectively. In 1995, he was granted the Dr. Eng. degree from the University of Electro-Communications, Tokyo, Japan. In 1996, he became a Research Assistant in the Department of Electronic Engineering, the University of Electro-Communications, where became an Associate Professor in 1997. From 1998 to 2008, he was an Associate Professor in the Department of Electrical and Electronic Systems, Saitama University, Japan. He was promoted to become a Professor at the same university in 2009. From 1985 to 1989, he was engaged in research on dielectric waveguides, resonators and leaky-wave antennas. From 1990 to 1997, he studied on computational electromagnetics, and the analytical and numerical modeling of various microwave and millimeter-wave transmission lines and circuits. His current research is mainly on the development of microwave and millimeter-wave devices and circuits, and the measurement of dielectric materials and high-temperature superconductors. He received a Japanese Government Graduate Scholarship from 1991 to 1993. He was granted the URSI Young Scientist Award in 1993. From 1994 to 1996, he was a Research Fellow of the Japan Society for the Promotion of Science (JSPS). He is a member of IEEE and a senior member of the IEICE. He is the Vice-President of the Technical Group on Electronics Simulation Technology of the Electronics Society, IEICE. He has served on the Editorial Board of IEEE Transactions on Microwave Theory and Techniques, the Review Board of IEEE Microwave and Wireless Components Letters, and the Review Board of IEICE Transactions on Electronics.